TOPICAL REVIEW

Nitrogen in chromium–manganese stainless steels: a review on the evaluation of stacking fault energy by computational thermodynamics

Linda Mosecker[1] and Alireza Saeed-Akbari[2]

[1] Department of Ferrous Metallurgy, RWTH Aachen University, Intzestrasse 1,
D-52072 Aachen, Germany
[2] Laboratory of Metal Physics and Technology, Swiss Federal Institute of Technology (ETH) Zurich,
Wolfgang-Pauli-Strasse 10, CH-8093 Zürich, Switzerland

E-mail: Linda.Mosecker@iehk.rwth-aachen.de

Abstract
Nitrogen in austenitic stainless steels and its effect on the stacking fault energy (SFE) has been the subject of intense discussions in the literature. Until today, no generally accepted method for the SFE calculation exists that can be applied to a wide range of chemical compositions in these systems. Besides different types of models that are used from first-principle to thermodynamics-based approaches, one main reason is the general lack of experimentally measured SFE values for these steels. Moreover, in the respective studies, not only different alloying systems but also different domains of nitrogen contents were analyzed resulting in contrary conclusions on the effect of nitrogen on the SFE. This work gives a review on the current state of SFE calculation by computational thermodynamics for the Fe–Cr–Mn–N system. An assessment of the thermodynamic effective Gibbs free energy, $\Delta G^{\gamma \to \varepsilon}$, model for the $\gamma \to \varepsilon$ phase transformation considering existing data from different literature and commercial databases is given. Furthermore, we introduce the application of a non-constant composition-dependent interfacial energy, $\sigma^{\gamma/\varepsilon}$, required to consider the effect of nitrogen on SFE in these systems.

Keywords: stacking fault energy, interfacial energy, nitrogen, Suzuki segregation, austenitic stainless steels

1. Introduction

The effect of nitrogen on the stacking fault energy (SFE) and the resultant deformation behavior in austenitic stainless chromium–manganese steels have been extensively discussed

in the literature [1–17]. However, intensive research has not lead to a general analysis which, besides the general lack of experimentally measured SFE values in that system, is mainly due to different domains of nitrogen contents and different alloying systems that are analyzed in the respective studies. In figure 1, the dependence of SFE on the nitrogen content in different reported systems is shown. In that regard, it has been reported that nitrogen increases the SFE in Fe–Cr–Mn [1, 2], Fe–(Mn)–N [3], Fe–Mn–Si–Al [4] and Fe–Cr–Mn–C [5, 6], or decreases
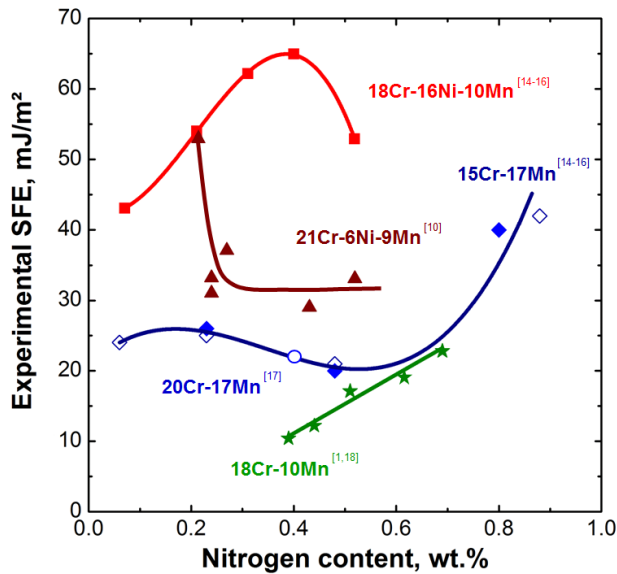
Figure 1. Experimentally measured SFE over nitrogen content in Fe–Cr–Ni–Mn and Fe–Cr–Mn systems.

the SFE in Fe–Cr–Ni–Mo [7], Fe–Cr–Mn [8], Fe–Cr–Ni [8, 9], Fe–Cr–Ni–Mn [10] and Fe–Mn–N [11] systems, but also results in a non-monotonous behavior of SFE as seen in the Fe–Cr–(Ni)–Mn system [12–16].

Nevertheless, the studies of Gavriljuk *et al* [16] and Petrov [14, 15] revealed that the effect of nitrogen in Fe–Cr–Mn is not comparable with that of the Fe–Cr–Ni system due to the differences in the free electron state resulting from the Ni–N and Mn–N interactions. Therefore, the reported SFEs in these works for the Fe–15Cr–17Mn system with nitrogen content of 0.06–0.88 wt% are the only available experimentally measured values in nickel-free austenitic stainless steels besides the works of Jandová *et al* [17] for the steel Fe–20Cr–17Mn–0.4N with a SFE of 22 mJ m^{-2} and Lee *et al* [1] in the system Fe–18Cr–10Mn with 0.33–0.69 wt% nitrogen that cover a wide range of nitrogen content.

In order to estimate the SFE in austenitic stainless steels with different chemical compositions, various methods using computational thermodynamics assessments [12, 14, 19–21], including the latest works by Curtze *et al* [22] and Roncery *et al* [23, 24], quantum mechanical first-principle approaches [3, 25, 26], and empirical equations—as recently proposed by Lee *et al* [18] for the Fe–Cr–Mn–CN system—based on experimental analysis [9, 27–29] have been investigated. A widely used approach to calculate an ideal SFE was proposed by Olsen and Cohen [30] which defines the required Gibbs free energy to form an intrinsic stacking fault by the movement of a single Shockley partial dislocation on a close packed plane. Since the motion of the partial dislocation occurs on every second plane, a hexagonal close packed (hcp) crystalline structure is formed with a thickness of two atomic layers. According to Adler *et al* [31], the core equation to calculate the SFE is

$$\text{SFE} = 2\rho\,\Delta G^{\gamma\to\varepsilon} + 2\sigma^{\gamma/\varepsilon}, \qquad (1)$$

where ρ is the molar surface density along {111} planes, $\Delta G^{\gamma\to\varepsilon}$ is the change of the molar Gibbs free energy due to the phase transformation of face cubic centered (fcc) austenite (γ) to hcp-ε-martensite, and $\sigma^{\gamma/\varepsilon}$ defines the interfacial energy of the λ/ε-interface that can vary within different alloying systems [32, 33]. Since nitrogen is known to be a strong austenite stabilizer and suppresses the formation of α'- or ε-martensite in the Fe–Cr–Mn system [1], a linear increase of the Gibbs free energy, $\Delta G^{\gamma\to\varepsilon}$, by alloying with nitrogen is observed. However, the reported non-monotonous dependence of SFE on nitrogen content (as seen in the Fe–Cr–Mn compositions of figure 1) can no longer be expressed by a linear relation to $\Delta G^{\gamma\to\varepsilon}$ as described by equation (1) where the interfacial energy is set constant.

This article gives a review on the current state of SFE calculation by computational thermodynamics for the Fe–Cr–Mn–N system. The thermodynamic data available in the literature and in software databases such as Thermo-Calc for the $\Delta G^{\gamma\to\varepsilon}$ model as a thermodynamic basis for the SFE calculation are evaluated. Based on equation (1), the two common methods for the SFE calculations in this system are validated by a number of investigated chemical compositions from literature with the given microstructures before and after deformation at room temperature as shown in table 1. It is proposed that in order to consider the effect of nitrogen on SFE, a composition-dependent description of the interfacial energy, $\sigma^{\gamma/\varepsilon}$, is required that has not yet been described in the literature.

2. Thermodynamic modeling of Gibbs free energy $\Delta G^{\gamma\to\varepsilon}$

In several works on the SFE calculation in the Fe–Mn–C system [32, 60–62] and also on austenitic stainless steels [22], the applied thermodynamic model for the calculation of an effective Gibbs free energy of the $\gamma\to\varepsilon$ phase transformation, $\Delta G^{\gamma\to\varepsilon}$, has been defined as a subregular solid solution model with ideal entropy of mixing which assumes the elements of a system to be in a random mixing. In the mentioned model, the interstitial elements like carbon or nitrogen have been considered to be in a substitutional solution without taking vacancies into account. As a consequence, the effect of interstitial elements is described insufficiently with respect to the thermal and furthermore, mechanical phase stability in the SFE calculation (figure 2). The SFE value defines the activation of transformation induced plasticity (TRIP) and twinning induced plasticity (TWIP) mechanisms and by that strongly influences the work-hardening behavior [62]. Above the TRIP/TWIP transition line, the activation of deformation twinning defines the variations and the levels of work-hardening rate diagrams. In this range of SFEs, lower SFE values result in the formation of finer twins, progressive decrease in the mean free path of dislocations by continuation of the plastic deformation referred to as the dynamic Hall–Petch effect, and cutting of dislocation substructures by twin boundaries [61]. While in the SFE range below the TRIP/TWIP transition line the $\gamma\to\varepsilon$-martensite and $\gamma\to\varepsilon\to\alpha$'-martensitic transformations are

Table 1. Chemical composition and microstructure before and after deformation of austenitic stainless steels reported in the literature.

Reference		Chemical composition (wt%)					Microstructure	
Author	Year	Cr	Mn	Ni	N	C	before deformation	after deformation
Remy and	1977	4.8	29.6	–	–	0.02	γ	$\gamma + \varepsilon_D$
Pineau [34]		5.0	28.2	–	–	0.01	γ	$\gamma + \varepsilon_D$
		5.1	31.3	–	–	0.01	γ	γ^T
Lenel and Knott [35]	1987	11.8	10.4	–	0.19	–	γ	$\gamma + \alpha'_D$
		13.4	10.2	–	0.23	–	γ	$\gamma + \alpha'_D$
		12.6	9.5	–	0.32	–	γ	$\gamma + \alpha'_D$
		12.7	9.1	–	0.22	–	γ	$\gamma + \alpha'_D$
		12.1	8.3	–	0.16	–	γ	$\gamma + \alpha'_D$
		11.8	8.3	–	0.18	–	γ	$\gamma + \alpha'_D$
		11.8	8.1	–	0.21	–	γ	$\gamma + \alpha'_D$
Nyilas and Obst [36]	1988	5.2	25.6	–	–	–	γ	γ
		5.2	25.6	–	0.06	0.02	γ	γ
		5.2	25.5	–	0.10	0.02	γ	γ
		8.5	39.8	–	0.28	0.06	γ	γ
		13.4	33.9	–	0.32	0.04	γ	γ
Kitamura *et al* [37]	1990	19.5	19.6	–	0.65	0.08	γ	γ
		20.1	19.2	–	0.73	0.07	γ	γ
Földéaki and	1992	18.3	19.0	0.2	0.57	0.10	γ	γ
Ledbetter [38]		18.8	18.8	0.1	0.8	0.01	γ	γ
		14.0	20.2	0.3	0.39	0.01	γ	γ
Ilola *et al* [8]	1996	22.2	12.3	0.4	0.97	0.02	γ	γ^T
Uggowitzer *et al* [39]	1996	18.2	19.0	1.2	0.61	0.08	γ	γ
Vogt *et al* [40]	1996	18.7	19.1	0.5	0.90	0.04	γ	γ
Onozuka *et al* [41]	1998	13.5	24.5	–	0.20	0.02	γ	γ
Tomota *et al* [42, 43]	1998	17.2	18.8	0.2	0.51	0.07	γ	γ
		19.1	19.4	0.4	0.84	0.05	γ	γ (planar slip)
Mills and Knutsen [44]	1998	19.0	10.0	0.8	0.63	0.03	γ	γ
Liu *et al* [45, 46]	1998/04	19.3	19.6	0.3	0.70	0.05	γ	γ
Sorokina and	1999	14.0	14.0	–	–	–	$\gamma + \varepsilon + \alpha'$	$\gamma + \alpha'$
Shlyamnev [47]		14.0	16.0	–	–	–	$\gamma + \varepsilon$	$\gamma + \alpha'_D$
		14.0	18.0	–	–	–	$\gamma + \varepsilon$	$\gamma + \varepsilon_D + \alpha'_D$
		14.0	22.0	–	–	–	γ	$\gamma + \varepsilon_D$
Okada *et al* [48]	2003	12.0	6.6	–	0.03	–	$\gamma + \varepsilon + \alpha' + \delta$	$\gamma + \varepsilon_D + \alpha'_D + \delta$
		12.5	11.3	–	0.15	0.01	$\gamma + \varepsilon + \alpha'$	$\gamma + \varepsilon_D + \alpha'_D$
		12.0	23.0	–	–	–	$\gamma + \varepsilon + \delta$	$\gamma + \varepsilon_D + \alpha'_D$
		12.0	30.3	–	0.07	0.01	$\gamma + \varepsilon + \delta$	$\gamma + \varepsilon_D + \alpha'_D$
Petrov [14, 15]	2003/05	15.0	17.0	–	0.23	–	γ	γ
		15.0	17.0	–	0.48	–	γ	γ
		15.0	17.0	–	0.88	–	γ	γ
Efros *et al* [49]	2004	18.0	18.0	–	0.50	0.07	γ	γ
		18.0	20.0	–	0.80	0.08	γ	γ (planar slip)
Jandová *et al* [17]	2004	19.8	17.4	0.1	0.40	0.06	γ	γ^T
Balitskii [50]	2004	18.3	19.1	–	0.62	0.05	γ	γ
Gavriljuk *et al* [16]	2006	15.0	17.0	–	0.23	–	γ	γ
		15.0	17.0	–	0.48	–	γ	γ
		15.0	17.0	–	0.80	–	γ	γ
Saller *et al* [2]	2006	14.0	20.0	1.0	0.30	< 0.04	γ	γ^T
		21.0	23.0	1.0	0.90	< 0.04	γ	$\gamma^{(T)}$ (planar slip)

Table 1. Continued.

Reference		Chemical composition (wt%)					Microstructure	
Author	Year	Cr	Mn	Ni	N	C	before deformation	after deformation
Riedner *et al* [51]	2008	21.0	23.1	1.5	0.88	0.04	γ	γ (planar slip)
Lee *et al* [52, 1]	2008/10	18.0	9.7	–	0.33	0.03	γ	$\gamma + \varepsilon_D + \alpha'_D$
Kim *et al* [53]	2009	17.8	9.7	–	0.39	0.03	γ	$\gamma + \varepsilon_D + \alpha'_D$
		18.1	9.7	–	0.44	0.03	γ	$\gamma + \varepsilon_D + \alpha'_D$
		17.7	9.6	–	0.51	0.03	γ	$\gamma^T + \varepsilon_D + \alpha'_D$
		18.6	10.0	2.1	0.53	0.02	γ	$\gamma^T + \varepsilon_D + \alpha'_D$
Hwang *et al* [54]	2011	18.5	9.5	0.4	0.58	0.04	γ	$\gamma^T(+\varepsilon_D)$
Lee *et al* [18]	2012	18.3	9.7	–	0.61	0.02	γ	$\gamma^T + \varepsilon_D$
Hwang *et al* [55]	2011	17.5	9.8	–	0.69	0.03	γ	γ^T
Milititsky *et al* [56]	2008	18.0	17.7	0.2	0.49	0.04	γ	γ^T
Dai *et al* [27]	2009	13.2	24.6	0.1	0.44	–	γ	γ^T
Terazawa *et al* [57]	2009	21.0	23.0	–	0.90	–	γ	γ (planar slip)
Yang and Ren [58]	2010	17.9	15.3	< 0.2	0.46	–	γ	γ
		21.0	23.0	< 0.3	0.97	–	γ	γ
Xu *et al* [59]	2011	18.7	12.5	–	0.55	0.05	γ	γ^T
Choi *et al* [29]	2011	20.3	5.0	0.2	0.10	0.02	$\gamma + \delta$	$\gamma + \alpha'_D + \delta$
		20.2	5.1	0.2	0.19	0.02	$\gamma + \delta$	$\gamma + \alpha'_D + \delta$
		20.1	5.0	0.2	0.28	0.02	$\gamma + \delta$	$\gamma + \alpha'_D + \delta$

γ — austenite, γ^T — mechanical twinning, $\gamma^{(T)}$ — minor twinning, ε — thermal hcp martensite, ε_D — deformation induced hcp martensite, α' — thermal bcc/bct martensite, α'_D — deformation induced bcc/bct martensite, δ — delta ferrite.
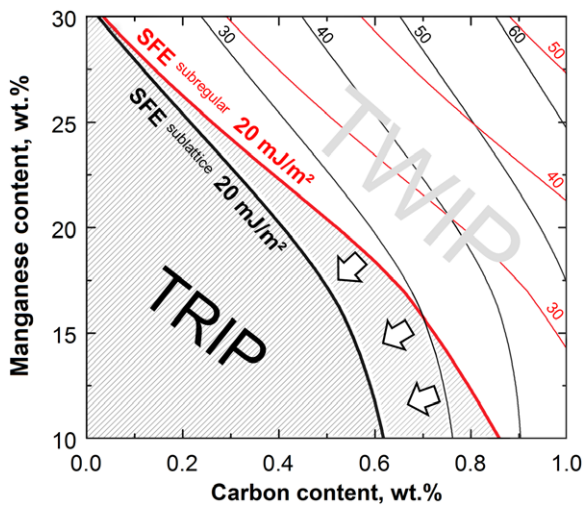
Figure 2. Thermodynamics-based SFE mechanism map of the Fe–Mn–C system calculated according to Saeed-Akbari *et al* [62] using the subregular model (red lines) and Djurovic *et al* [63] using the sublattice model (black lines).

possible, resulting in a markedly high work-hardening rate at low strains but sudden drop of work-hardening rate until fracture.

Moreover, the employed interaction parameter, $\Omega^{\gamma \to \varepsilon}$, for the calculation of the excess Gibbs free energy in the subregular model considers only the second order, binary interactions for each pair of system constituents multiplied with the relevant molar fractions. The importance of the interaction between the alloying elements in quaternary

Fe–Cr–Ni–X alloys (where X = Mn, Cu, Nb) was intensively discussed in the work by Lu *et al* [64] using a quantum-mechanical all-electron first principle method. It was found that due to the interaction of the alloying elements, the effect of each single element on the SFE can change dramatically and therefore needs to be taken into account for SFE calculations using computational thermodynamics. With it, particularly in higher ordered systems with more than two components, applying the subregular solid solution model for the calculation of $\Delta G^{\gamma \to \varepsilon}$ can be seen as an oversimplification. Hence, in most CALPHAD works, a generally accepted thermodynamic model that accounts for the real crystalline structure is used. In the so-called *sublattice model*, elements that are sufficiently different can occupy different sublattices and vacancies are treated as separate elements in the interstitial sublattice while random mixing in each sublattice is assumed [65]. The application of the sublattice model for the $\Delta G^{\gamma \to \varepsilon}$ calculation in the SFE equation (1) is already known from the works by Ferreira and Müllner [21] in the Fe–Cr–Ni system, Roncery *et al* [23, 24] in the Fe–Cr–Mn–N using Thermo-Calc software, but also by Nakano and Jacques [33, 66] in the Fe–Mn–C system. Above all, the Fe–Mn–C austenitic steels are one of the currently well-established austenitic high-Mn systems [67]. Besides the SFE calculations performed by Saeed-Akbari *et al* [62] using the subregular model, the latest improvement of the thermodynamic parameter employing the sublattice model was proposed by Djurovic *et al* [63] in this system. As can be seen from the corresponding SFE mechanism map in figure 2 as a function of manganese and carbon, the effect

of the interstitial element carbon on the SFE and by that on the austenite phase stability strongly depends on the applied subregular or sublattice model.

In the early 1990s, Qui [68] adopted the sublattice model to the quaternary Fe–Cr–Mn–N system in order to predict the thermodynamic phase stabilities and phase-relations as a function of nitrogen content. Since then, no further adjustment of the model has been done, even though different combinations of thermodynamic parameter and their interpretation can be found in literature. In the following, the calculation of $\Delta G^{\gamma \rightarrow \varepsilon}$ is described and analyzed on the basis of the model by Qui [68] taking into account the additional findings from the literature, giving an overview of the current state of the thermodynamic model.

2.1. Thermodynamic two-sublattice model

Introduced by Hillert and Staffansson [69] in the two-sublattice model, the observed fcc and hcp phases for the calculation of an effective Gibbs free energy of the $\gamma \rightarrow \varepsilon$ phase transformation, $\Delta G^{\gamma \rightarrow \varepsilon}$, are treated as interstitial solutions of nitrogen in the γ-Fe and ε-Fe, respectively. In the evaluation of Cr–N, Mn–N and Fe–N binary systems, the M_2N phase is regarded as a nitrogen-rich solution within the hexagonal M. Therefore, the interstitial solution of nitrogen in the hcp phase of a metal can be described by the same thermodynamic parameters as the M_2N nitride. The M_2N phase is approximated in the form of $(Cr, Fe, Mn)_1(N, Va)_{0.5}$ with the site occupancy of 1:0.5, where it is assumed that the interstitial sites are never simultaneously occupied [70], and $Cr_1va_{0.5}$, $Fe_1va_{0.5}$ and $Mn_1va_{0.5}$ represent pure chromium, iron and manganese in the hcp state, respectively [71]. In the fcc phase, $(Cr, Fe, Mn)_1(N, Va)_1$, the number of sites in each sublattice is equal to one. The Gibbs free energy of every phase, G^{Φ}, can be then calculated separately, with the site numbers in each sublattice of $a = c = 1$ for fcc and $a = 1$, $c = 0.5$ for hcp, as follows:

$$G^{\Phi} = \sum_i y_i (y_{va}^{\circ} G_{i:va}^{\Phi} + y_N^{\circ} G_{i:N}^{\Phi})$$
$$+ \left[aRT \sum_i y_i \ln y_i + cRT (y_N \ln y_N + y_{va} \ln y_{va}) \right]$$
$$+ G_{excess}^{\Phi} + G_{magn}^{\Phi}, \quad (2)$$

where

$$G_{excess}^{\Phi} = y_N y_{va} \sum_{i=1} y_i L_{i:N;va}^{\Phi}$$
$$+ y_N y_{va} \sum_{i=1} \sum_{j=i+1} y_i y_j L_{i;j:N;va}^{\Phi}$$
$$+ \sum_{i=1} \sum_{j=i+1} y_i y_j (y_N L_{i;j:N}^{\Phi} + y_{va} L_{i;j:va}^{\Phi})$$
$$+ y_{Cr} y_{Fe} y_{Mn} (y_N L_{Cr,Fe,Mn:N}^{\Phi} + y_{va} L_{Cr,Fe,Mn:va}^{\Phi}) \quad (3)$$

with $i, j =$ Fe, Mn, Cr. The first term of the Gibbs free energy refers to the ideal reference state of a solution that defines

the Gibbs energy of the interactions between neighboring atoms of elements in different sublattices [65], while the second term is the ideal entropy of mixing. The terms G_{excess}^{Φ} and G_{magn}^{Φ} represent the contributions to the Gibbs energy due to the interactions between different elements and the magnetic ordering, respectively. The interaction parameter, L, in the excess Gibbs energy term, G_{excess}^{Φ}, is composition- and temperature-dependent according to the Redlich–Kister [72] power series. The magnetic contribution to Gibbs free energy, G_{magn}^{Φ}, is described by using the approach of Hillert and Jarl [73] formulated as a Taylor expansion of the formalism proposed by Inden [74] restricted to the third term. The critical temperature for the anti-ferromagnetic ordering, $^{\circ}T_{Neel}^{\Phi}$, and the total magnetic entropy, $^{\circ}\beta^{\Phi}$, are expressed as functions of temperature and composition. It is assumed that nitrogen has no effect on the magnetic term of the Gibbs free energy of the fcc and hcp phases [12, 66, 75].

All thermodynamic parameters available in the literature for the $\Delta G^{\gamma \rightarrow \varepsilon}$ calculation are summarized in table 2. Evaluated from the binary systems Cr–N [76], Fe–N [76] and Mn–N [77], the Gibbs free energies, $^{\circ}G_{i:N}^{\Phi}$, represent the state of energy in which all interstitial sites are filled with nitrogen. The parameters $^{\circ}G_{i:Va}^{\Phi}$ denote the Gibbs free energy of the pure elements in a hypothetically nonmagnetic state originated from the scientific group thermodata Europe (SGTE) database for pure elements after Dinsdale [78]. The variables $y_{i,j}$ are the site fractions of the components i, j in the equal sublattice. For the substitutional sublattice,

$$y_{i,j} = \frac{x_{i,j}}{(1 - x_N)} \quad (4)$$

and for nitrogen the interstitial sublattice with vacancies is defined as

$$y_N = \frac{x_N}{c(1 - x_N)}, \quad (5)$$

where x denotes the mole fraction of each element in the system. The site fractions are correlated as follows:

$$y_{Fe} + y_{Mn} + y_{Cr} = 1, \quad (6)$$

$$y_N + y_{va} = 1. \quad (7)$$

The ternary interaction parameter $L_{Cr,Fe:N}^{(fcc)}$ was introduced by Frisk [71] to improve the solubility limits of nitrogen in austenite at high pressures by fitting the experimental data from Feichtinger et al [79]. However, using this parameter in the $\Delta G^{\gamma \rightarrow \varepsilon}$ calculation, the experimental results from Lee et al [1, 18, 52] and Hwang et al [54] in the Fe–18Cr–10Mn system with higher nitrogen contents (see table 1) cannot be described. For these steels, using the $L_{Cr,Fe:N}^{(fcc)}$ by Frisk [71], the model predicts a highly stable austenite phase, although after deformation, the non-deformed γ-phase was transformed to ε- and α'-martensite (figure 3(a)). Previous results of Dimova et al [80] on nitrogen solubility in Fe–22Cr–3Mn and Fe–21Cr–5Mn confirm considerably lower values as calculated for fcc Fe–Cr by Frisk [71]. Since there are no further thermodynamic data available in the literature to reproduce these experimental observations, $L_{Cr,Fe:N}^{(fcc)}$ should be approximated by setting it equal to the parameter for

Table 2. Thermodynamic parameter for the Fe–Cr–Mn–N system used from literature[a].

fcc phase	2 sublattice, sites 1:1, constituents $(Cr, Fe, Mn)_1(N, Va)_1$	Reference
$°G$(fcc) Fe:Va	$°G$(bcc) Fe:Va $-1462.4 + 8.282T - 1.15T \ln T + 6.410^{-4}T^2$	[88]
$°G$(fcc) Cr:Va	$°G$(bcc) Cr:Va $+ 7284 + 0.163T$	[89]
$°G$(fcc) Mn:Va	$-3439.3 + 131.884T - 24.5177T \ln T - 0.006T^2 + 69600T^{-1}$	[90]
$°G$(fcc) Fe:N	$°G$(bcc) Fe:Va $+ 0.5°G$(gas)$N_2 - 37460 + 375.42T - 37.6T \ln T$	[76]
$°G$(fcc) Cr:N	$°G$(bcc) Cr:Va $+ 0.5°G$(gas)$N_2 - 124460 + 142.16T - 8.5T \ln T$	[76]
$°G$(fcc) Mn:N	$-75940 + 292.226T - 50.294T \ln T + 265051T^{-1}$	[77]
L(fcc) Fe:N,Va	$-26\,150$	[91]
L(fcc) Cr:N,Va	$20\,000$	[76]
L(fcc) Mn:N,Va	$-69698 + 11.5845T$	[77]
L(fcc) *Cr,Fe:N*	$-128930 + 86.49T + 24330(y_{Cr} - y_{Fe})$	[71]
L(fcc) Cr,Fe:N	$12826 - 19.48T$	[71]
L(fcc) Cr,Fe:Va	$10833 - 7.477T - 1410(y_{Cr} - y_{Fe})$	[89]
L(fcc) Cr,Fe:N,Va	$-162\,516$[b]	[71]
L(fcc) Cr,Fe:N,Va	0	[71]
L(fcc) Cr,Mn:N	$-21\,237$	[70]
L(fcc) Cr,Mn:Va	$-19\,088 + 17.5423T$	[81]
L(fcc) Fe,Mn:N	$53\,968 - 38.102T - 28787(y_{Fe} - y_{Mn})$	[92]
L(fcc) Fe,Mn:Va	$-7762 + 3.865T - 259(y_{Fe} - y_{Mn})$	[93]
L(fcc) Cr,Fe,Mn:N	$-118\,000$	[68]
L(fcc) Cr,Fe,Mn:Va	$6715 - 10.3933T$	[81]
β(fcc)	$-2.46y_{Cr}y_{Va} - 2.1y_{Fe}y_{Va} - 1.86y_{Mn}y_{Va}$	[68]
Neel T (fcc)	$-1109y_{Cr}y_{Va} - 201y_{Fe}y_{Va} - 1620y_{Mn}y_{Va} - y_{Fe}y_{Mn}y_{Va}[2282 + 2068(y_{Fe} - y_{Mn})]$	[68]

hcp phase	2 sublattice, sites 1:1, constituents $(Cr, Fe, Mn)_1(N, Va)_1$	
$°G$(hcp) Fe:Va	$°G$(fcc) Fe:Va $-2243.4 + 4.3095T$	[88]
$°G$(hcp) Cr:Va	$°G$(bcc) Cr:Va $+ 4438$	[89]
$°G$(hcp) Mn:Va	$°G$(fcc) Mn:Va $- 1000 + 1.123T$	[94]
$°G$(hcp) Fe:N	$°G$(bcc) Fe:Va $+ 0.25°G$(gas)$N_2 - 12015 + 37.98T$	[76]
$°G$(hcp) Cr:N	$°G$(bcc) Cr:Va $+ 0.25°G$(gas)$N_2 - 65760 + 64.69T - 3.93T \ln T$	[76]
$°G$(hcp) Mn:N	$-60607 + 211.1807T - 37.7331T \ln T + 129442T^{-1}$	[77]
L(hcp) Fe:N,Va	$10345 - 19.71T - (11130 - 11.84T)(y_N - y_{Va})$	[76]
L(hcp) Cr:N,Va	$21120 - 10.61T - 6204(y_N - y_{Va})$	[76]
L(hcp) Mn:N,Va	$-7194 - 5.2075T - (11810 - 6.9538T)(y_N - y_{Va})$	[77]
L(hcp) Cr,Fe:N	$12826 - 19.48T$	[71]
L(hcp) Cr,Fe:Va	$10833 - 7.477T$	[71]
L(hcp) Cr,Mn:N	$-42187 + 32.48T$	[70]
L(hcp) Cr,Mn:Va	$-19088 + 17.5423T$	[70]
L(hcp) Fe,Mn:N	*no data available*	[92]
L(hcp) Fe,Mn:Va	$-5582 + 3.865T + 273(y_{Fe} - y_{Mn})$	[93]
L(hcp) Cr,Fe,Mn:N	-185400	[68]
L(hcp) Cr,Fe,Mn:Va	34600	[68]
L(hcp) Fe:N,Va	$10345 - 19.71T - (11130 - 11.84T)(y_N - y_{Va})$	[76]
β(hcp)	$-2.46y_{Cr}y_{Va} - 1.86y_{Mn}y_{Va}$	[81]
Neel T (hcp)	$-1109y_{Cr}y_{Va} - 1620y_{Mn}y_{Va}$	[81]

bcc phase	2 sublatices, sites 1:3, Constituents $(Cr, Fe, Mn)_1(N, Va)_3$	
$°G$(bcc) Fe:Va	$1225.7 + 124.134T - 23.5143T \ln T - 0.00439752T^2 - 5.89269\ 10^{-8}T^3 + 77358.5T^{-1}$	[88]
$°G$(bcc) Cr:Va	$-8856.94 + 157.48T - 26.908T \ln T + 1.89435\ 10^{-3}T^2 - 1.47721\ 10^{-6}T^3 + 139250T^{-1}$	[95]
$°G$(bcc) Fe:N	$°G$(bcc)Fe:Va $+ 0.75°G$(gas)$N_2 + 93562 + 165.07T$	[76]
$°G$(bcc) Cr:N	$°G$(bcc)Cr:Va $+ 0.75°G$(gas)$N_2 + 311870 + 29.12T$	[76]

[a] All values are given in SI units J, mol and K.

[b] Parameter only exists for the fcc phase [71].

the hcp phase, $L_{Cr,Fe:N}^{(hcp)}$ (figure 3(c)) in order to adjust the $\Delta G^{\gamma \rightarrow \varepsilon} = 0$ transition line. This assumption can be adopted from Frisk [71] for the ternary parameter $L_{Cr,Mn:va}^{(hcp)}$ that was set equal to $L_{Cr,Mn:va}^{(fcc)}$ from Lee [81]. Furthermore, the parameter $L_{Cr,Fe:N,va}^{(fcc)}$ as evaluated by Frisk [71] to adjust the miscibility gap of austenite and CrN nitride should be set zero due to

its strong influence on the nitrogen solubility in austenite and thereby the stability of the γ-phase (figure 3(b)).

2.2. Model validation with experimental data

The calculated Gibbs free energy $\Delta G^{\gamma \rightarrow \varepsilon}$ maps at 300 K for the Fe–Cr–Mn–N system with the thermodynamic model by
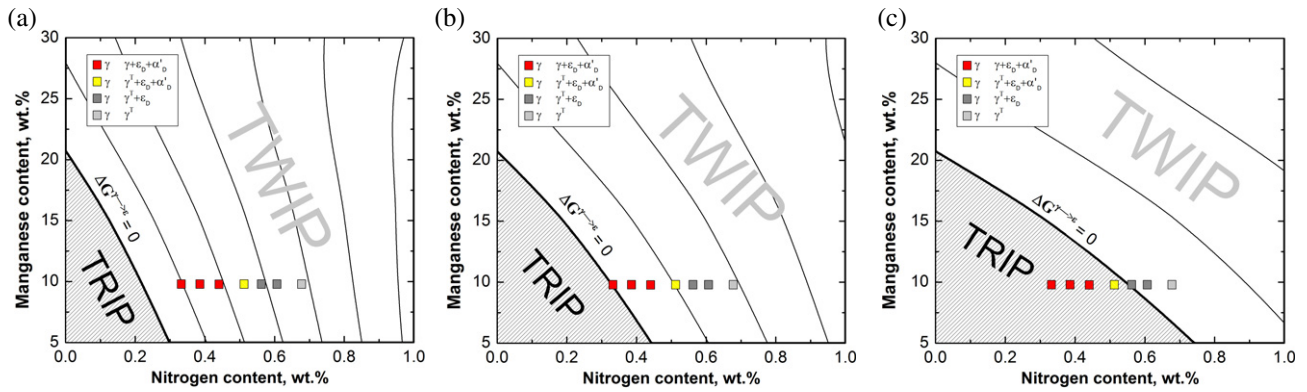
Figure 3. Calculated $\Delta G^{\gamma \to \varepsilon}$ maps at 300 K within the Fe–18Cr–Mn–N [1, 18, 52, 54] system (a) with $L_{Cr,Fe:N}^{(fcc)}$ [71] and $L_{Cr,Fe:N,Va}^{(fcc)}$ [71], (b) with $L_{Cr,Fe:N}^{(fcc)}$ [71] and $L_{Cr,Fe:N,Va}^{(fcc)} = 0$ [71] and (c) with $L_{Cr,Fe:N}^{(fcc)} = L_{Cr,Fe:N}^{(hcp)}$ [71] and $L_{Cr,Fe:N,Va}^{(fcc)} = 0$ [71].
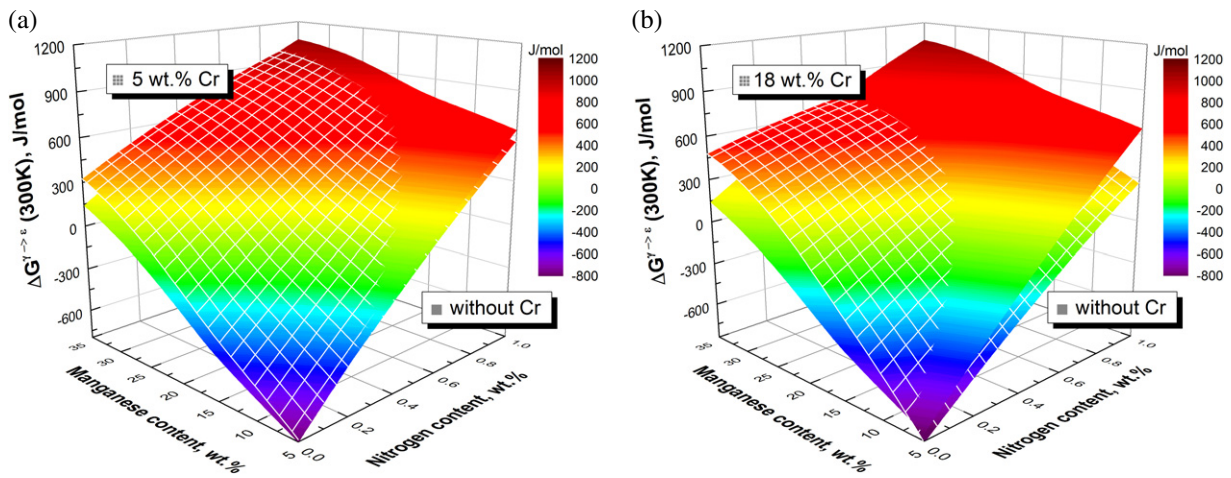
Figure 4. Calculated $\Delta G^{\gamma \to \varepsilon}$ maps of Fe–Cr–Mn–N alloys showing the effect of chromium: (a) 5 wt% Cr and (b) 18 wt% Cr.

Qui [68] considering the works of Frisk [71], are presented in figure 4 with constant chromium content. Increasing manganese and nitrogen stabilizes the fcc phase [82–84] which consequently results in an increase of $\Delta G^{\gamma \to \varepsilon}$ and a shift of the $\Delta G^{\gamma \to \varepsilon} = 0$ transition line to lower levels.

By adding chromium to the system, the fcc phase is stabilized at lower nitrogen contents, as can be confirmed from the experimental results of Bracke *et al* [5,6] in Fe–(0–10 wt%)Cr–Mn–N–C, while at higher nitrogen contents, the hcp phase becomes more favorable. This trend can be explained by the thermodynamic description of the hcp phase by Cr$_2$N nitride as mentioned earlier. Accordingly, with increasing nitrogen in the system, chromium prefers to form a Cr$_2$N nitride than staying in the fcc solid solution. The preference of chromium to form a nitride will be enhanced both with increasing chromium and nitrogen in Fe–Mn by rising the chromium content from 5 wt% (figure 4(a)) to 18 wt% (figure 4(b)).

The thermodynamic calculation of $\Delta G^{\gamma \to \varepsilon}$ is verified by a number of chemical compositions in the Fe–Cr–Mn–N system available in the literature with the given microstructures before and after deformation at room temperature summarized in table 1. For all steels where the Gibbs energy is estimated to be positive ($\Delta G^{\gamma \to \varepsilon} > 0$) in

the described model, the microstructures before and after deformation at room temperature were reported to be fully austenitic (figure 5).

Whenever the initial austenitic microstructure was transformed to ε_D- and/or α_D'-martensite by deformation, the calculated $\Delta G^{\gamma \to \varepsilon}$ values were negative. In this regard, the prediction of the available microstructural phases in the non-deformed as-received state—to be fully austenitic or partially martensitic (thermal ε- and/or α'-martensite)—is not possible since the composition-dependence of the driving force for the $\gamma \to \varepsilon$ transformation is still not clearly described in the literature. Recent works by Nakano [66] and Djurovic *et al* [63] suggest an increasing effect of carbon on the mentioned driving force in Fe–Mn alloys. Lee and Choi [85] reported an increasing driving force for $\gamma \to \varepsilon$ martensitic transformation in Fe–(14–26 wt%)Mn with increasing manganese content, while the experimental measurements of A_s and M_s-temperatures in Fe–Mn by Cotes *et al* [83] showed no dependence of the driving force on manganese content, which is consistent with Ishida's [86] reports. In earlier works, the driving force for $\gamma \to \varepsilon$ transformation was also found to be decreasing with the manganese content [87], which was confirmed by Nakano [66] for Fe–Mn–C alloys with 10–35 wt%
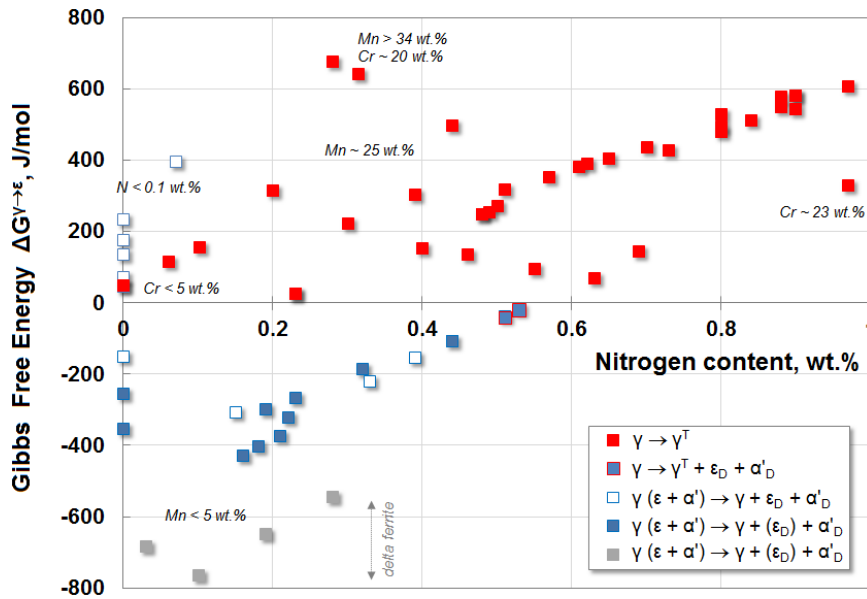
Figure 5. Calculated effective Gibbs free energy, $\Delta G^{\gamma \to \varepsilon}$, as function of nitrogen content for the examined steels with the chemical compositions from table 1 in the Fe–Cr–Mn–N system.

manganese. However, further research is required on this topic since the current thermodynamic databases have a shortage of appropriate parameters, especially in highly alloyed systems. In certain systems, this condition leads to inconsistencies in the prediction of thermodynamic phase stabilities. As an example, in most of the reviewed steels with nitrogen contents lower than 0.1 wt%, the Gibbs free energy, $\Delta G^{\gamma \to \varepsilon}$, was positive, which means that thermodynamically, the formation of ε-martensite was impossible, even though ε_D- or α'_D-martensite were observed in the microstructure after deformation. Furthermore, manganese contents lower than 5 wt% resulted in the occurrence of delta ferrite up to 60 vol% in the as-received microstructure [29]. Overall, considering the range of chemical composition for the examined steels, the validity of the current model can be set to the following conditions: nitrogen: 0.1–1.0 wt%, chromium: 0–25 wt%, and manganese: 5–30 wt%.

3. Stacking fault energy in the Fe–Cr–Mn–N system

### 3.1. Thermodynamic modeling of SFE

Early investigations by Müllner *et al* [7] were carried out to characterize the microstructure evolution in austenitic nitrogen-alloyed and nitrogen-free steels during deformation. It was observed that independent of presence or lack of nitrogen within the considered systems, two main mechanisms, namely, planar dislocation glide, promoted by chromium-nitrogen short-range ordering [96–99], and mechanical twinning affect the plastic deformation. As reported by Petrov *et al* [14, 15], in more dilute solutions, nitrogen decreases the SFE. Hence, increasing the nitrogen content up to ~0.4 wt% not only results in decreasing the critical strain and enhances the critical stress for the onset of mechanical twinning, but also induces mechanical twinning at a fine scale in more positions in the microstructure.

Müllner *et al* [7] justified this observation based on the increasing effect of nitrogen on the local dislocation density, consequently affecting the distribution of active glide planes.

An explanation of this phenomenon was also given in the works of Gavriljuk *et al* [99–101]. Within the fcc iron lattice, nitrogen occurs as an interstitial element in solid solution, preferentially occupying octahedral sites [100]. In the vicinity of the nitrogen atoms, the concentration of s-electrons in the fcc iron increases, as was shown by *ab initio* calculations [101] and experimental studies on the electronic structure [99]. In the surroundings of the nitrogen atoms, the free electrons rearrange such that the energy of elastic distortions in the crystal lattice decreases [102]. The local electron density was shown to have a major influence on the dislocation interactions with nitrogen and can be attributed to the SFE in Fe–Cr–Mn alloys [101]. According to these results, the initial decrease of SFE in more dilute solutions due to the Suzuki segregation of interstitial nitrogen atoms to dislocations and stacking faults leads to the formation of locked dislocation barriers. At higher nitrogen contents, the SFE increases as the local segregation of nitrogen atoms becomes less effective. In that regard, the dependence of SFE on the nitrogen content has been reported to be strongly affected by the competition between the average nitrogen concentration in the bulk and the possible amount of segregated interstitials to the stacking faults. Hence, in order to calculate the SFE in the Fe–Cr–Mn–N system, the role of nitrogen segregation needs to be taken into account.

Using the general approach from equation (1) to calculate an ideal SFE, the interfacial energy $\sigma^{\gamma/\varepsilon}$ is usually set as a constant value of 10 mJ m^{-2} [30] giving a linear relationship between the $\Delta G^{\gamma \to \varepsilon}$ and SFE. According to Saeed-Akbari *et al* [32] the $\sigma^{\gamma/\varepsilon}$ varies depending on different systems and studies between 5–27 mJ m^{-2} mainly for Fe–Mn–(Al,Si)–C, and in the work by Roncery *et al* [23] the SFE calculations for Fe–Cr–Mn–CN alloys were performed with an $\sigma^{\gamma/\varepsilon}$
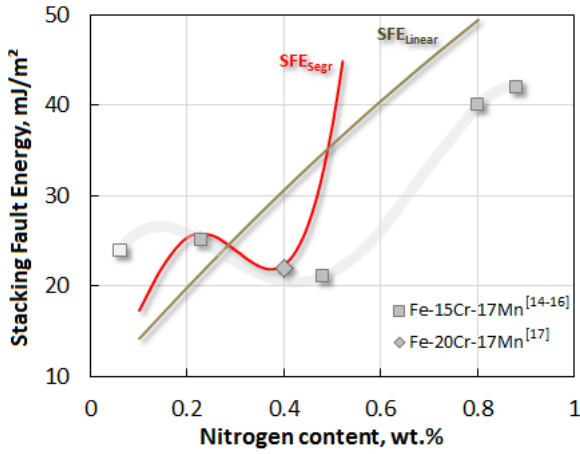
Figure 6. Calculated SFEs using different approaches: SFE$_{linear}$ from equation (1) and SFE$_{segr}$ from equation (8) with $\sigma^{\gamma/\varepsilon} = 4\,\mathrm{mJ\,m^{-2}}$ in comparison with the experimental results.

Figure 7. Interaction energy of nitrogen with dislocations in fcc iron alloys [12, 105] as function of nitrogen concentration.

of $5\,\mathrm{mJ\,m^{-2}}$. Using a constant $\sigma^{\gamma/\varepsilon}$ of $4\,\mathrm{mJ\,m^{-2}}$, the as-determined SFE$_{linear}$ values for Fe–15Cr–17Mn as a function of nitrogen content are shown in figure 6. In comparison with the experimentally measured SFE in the Fe–15Cr–17Mn [14–16] and Fe–20Cr–17Mn [17] systems, the SFE$_{linear}$ is not representing the non-monotonous trend of SFE versus nitrogen content. The measurement of SFE in the referred works was performed using the bright-field weak beam transmission electron microscopy (TEM) technique to determine three-fold extended dislocation nodes. The final values of SFE$_{TEM}$ were obtained using the model proposed by Brown and Thölén [103].

Correspondingly, two main approaches can be used to associate the effect of nitrogen segregation in equation (1):

(1) Using a constant interfacial energy, $\sigma^{\gamma/\varepsilon}$, where a segregation term $\Delta G_{segr}^{\gamma \to \varepsilon}$ is added to the Gibbs free energy, $\Delta G^{\gamma \to \varepsilon}$, as proposed by Ishida [19] and Yakubtsov *et al* [12]:

$$\mathrm{SFE}_{segr} = 2\rho(\Delta G^{\gamma \to \varepsilon} + \Delta G_{segr}^{\gamma \to \varepsilon}) + 2\sigma_{const}^{\gamma/\varepsilon}. \quad (8)$$
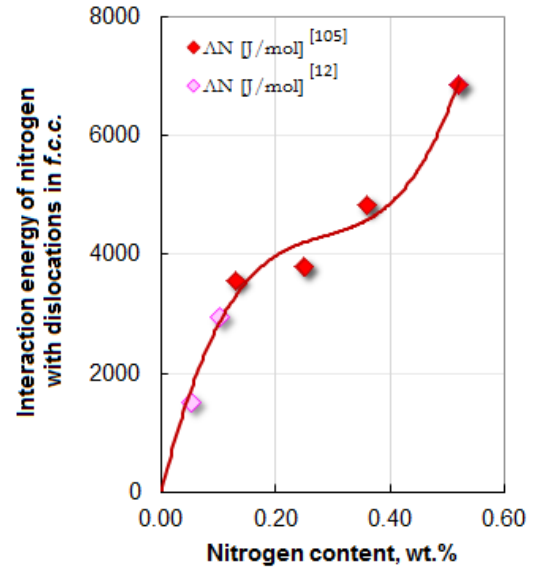
(2) Assuming the interfacial energy as non-constant value, where $\sigma_{comp}^{\gamma/\varepsilon}$ is defined as a composition-dependent parameter, as proposed in this work:

$$\mathrm{SFE}_{FIT} = 2\rho \Delta G^{\gamma \to \varepsilon} + 2\sigma_{comp}^{\gamma/\varepsilon}, \quad \text{where } \sigma_{comp}^{\gamma/\varepsilon}$$
$$= f(\mathrm{Fe, Mn, Cr, N}). \quad (9)$$

The molar surface density ρ in equations (1), (8) and (9) can be calculated after Allain *et al* [60] with a geometrical-dependence expressed by the lattice parameter, a_γ, of austenite. For the nickel-free austenitic stainless steels, the following composition-dependent equation by Srinivas and Kutumbarao [104] can be used to calculate a_γ:

$$a_\gamma \,(\mathrm{nm}) = 0.3578 + 0.00006x_{Cr} + 0.000095x_{Mn}$$
$$+ 0.0033x_C + 0.0029x_N, \quad (10)$$

where x_i is the molar fraction of element i in the alloying system. In the following, these two methods will be discussed.

3.2. Calculation of SFE considering $\Delta G_{segr}^{\gamma \to \varepsilon}$

As introduced by Ishida [19], the segregation term $\Delta G_{segr}^{\gamma \to \varepsilon}$ can be formulated (equation 11) as a sum of the chemical free energy $\Delta G_{chem}^{\gamma \to \varepsilon}$ due to Suzuki segregation from equation (12), the surface free energy $\Delta G_{surf}^{\gamma \to \varepsilon}$ due to the difference in concentration of nitrogen between matrix and stacking faults from equation (13), and the elastic free energy $\Delta G_{elast}^{\gamma \to \varepsilon}$ which is related to the segregation of substitutional and interstitial elements that have different atomic sizes, estimated to be negligible [19]:

$$\Delta G_{segr}^{\gamma \to \varepsilon} = \Delta G_{chem}^{\gamma \to \varepsilon} + \Delta G_{surf}^{\gamma \to \varepsilon} + (\Delta G_{elast}^{\gamma \to \varepsilon}) \quad (11)$$

with

$$\Delta G_{chem}^{\gamma \to \varepsilon} = RT \sum x_N \ln \frac{x_{s(N)}}{x_N}, \quad (12)$$

$$\Delta G_{surf}^{\gamma \to \varepsilon} = \frac{1}{4} \Lambda_N \left(x_{s(N)} - x_N\right)^2, \quad (13)$$

where

$$x_{s(N)} = \left[1 + \frac{(1 - x_N)}{x_N} \exp\left(\frac{-\Lambda_N}{RT}\right)\right]^{-1}. \quad (14)$$

The parameter x_N and $x_{s(N)}$ representing the concentration of nitrogen in the bulk and at the stacking faults, respectively. While Ishida [19] assumed the contribution of nitrogen segregation $\Delta G_{segr}^{\gamma \to \varepsilon}$ not to be significant, in the work of Yakubtsov *et al* [12] the interaction of nitrogen with dislocations and the resultant segregation to stacking faults were included in the model. The calculated SFE$_{segr}$ for Fe–15Cr–17Mn with a constant $\sigma^{\gamma/\varepsilon} = 4\,\mathrm{mJ\,m^{-2}}$ are shown in figure 6. In order to estimate the segregation of nitrogen to the stacking faults, mainly considered in the $\Delta G_{chem}^{\gamma \to \varepsilon}$ (equation 12) and $\Delta G_{surf}^{\gamma \to \varepsilon}$ (equation 13) terms, the interaction values of nitrogen atoms with dislocations Λ_N were employed in the model, since the required interaction energies between
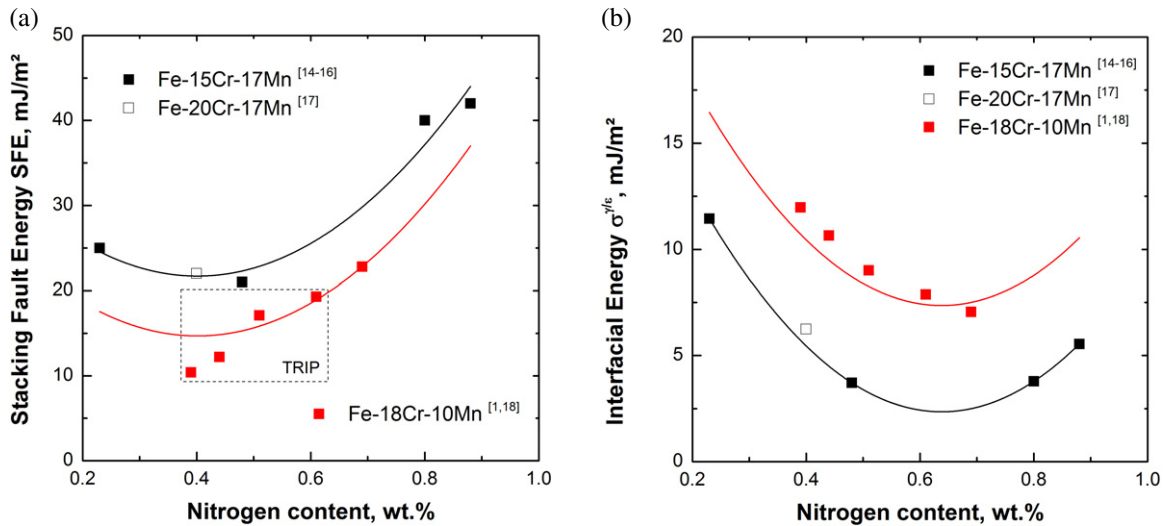
Figure 8. Polynomial description of (a) experimentally determined SFE values and (b) derived interfacial energy, $\sigma^{\gamma/\varepsilon}$, from Fe–15Cr–17Mn [14–16], Fe–20Cr–17Mn [17] and Fe–18Cr–10Mn [1, 18].
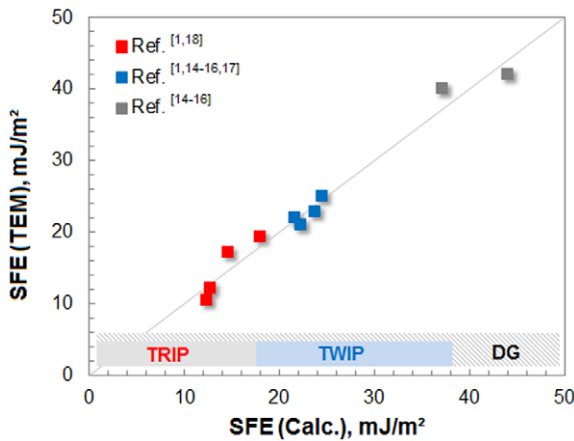
Figure 9. Comparison of experimental and calculated SFE in the Fe–Cr–Mn–N system. DG stands for the (planar) dislocation glide.
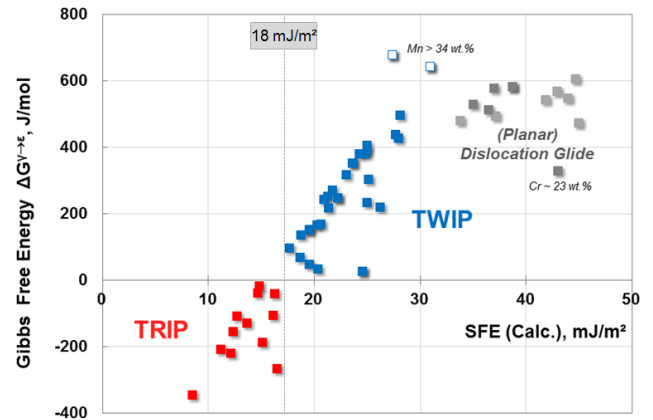
Figure 10. Calculated effective Gibbs free energy, $\Delta G^{\gamma \to \varepsilon}$, versus SFE values for the examined steels with the chemical compositions from table 1 in the Fe–Cr–Mn–N system.

nitrogen and stacking faults are not available [12]. The interaction values Λ_N were taken from the experimental approximations by Gavrilljuk *et al* [105] in the range of 0.13–0.52 wt% nitrogen and extrapolated by Yakubtsov *et al* [12] to 0–0.13 wt% nitrogen, as shown in figure 7. In the lower range of nitrogen contents, the calculated SFE$_{segr}$ matches the experimentally found SFE values, reproducing the drop of SFE due to nitrogen segregation (see figure 6).

However, with increasing nitrogen contents above ∼0.4 wt%, the model deviates from the experimental results. The reason might be explained by the applied interaction energies, Λ_N, that are limited to 0.52 wt% nitrogen content and because of that, the pertinency to the SFE at higher nitrogen contents is observed. On the other hand, the model was capable of predicting the SFE in Fe–Cr–Ni system in the work of Yakubtsov *et al* [12], which is, however, not comparable with the Fe–Cr–Mn system, as the interaction between nitrogen and substitutional elements changes depending on the available elements such as nickel or manganese [16, 106, 107].

3.3. Calculation of SFE considering $\sigma^{\gamma/\varepsilon}$ as non-constant

Published data concerning the dependence of $\sigma^{\gamma/\varepsilon}$ on the chemical composition in the Fe–Cr–Mn–N system have not been available until now. By adopting an experimental approximation of $\sigma^{\gamma/\varepsilon}$ after Olsen and Cohen [30] to estimate $\sigma^{\gamma/\varepsilon}$ based on equation (9), a non-monotonous composition-dependent description of the $\sigma^{\gamma/\varepsilon}$ for the Fe–(Cr)–Mn–N system can be proposed. Therefore, the experimentally measured SFE in the Fe–15Cr–17Mn [14–16] and Fe–20Cr–17Mn [17] systems, and another system investigated by Lee *et al* [1, 18] with 7 wt% less manganese, Fe–18Cr–10Mn, were used, representing the increasing effect of manganese on SFE [32, 61]. In figure 8, the corresponding polynomial to the experimental SFEs and the derived $\sigma^{\gamma/\varepsilon}$ are shown.

The effect of nitrogen on $\sigma^{\gamma/\varepsilon}$ is produced as a non-monotonous trend reflecting the influence of nitrogen segregation on SFE (figure 8(b)). Although the chromium content of the Fe–20Cr–17Mn was much higher than in the
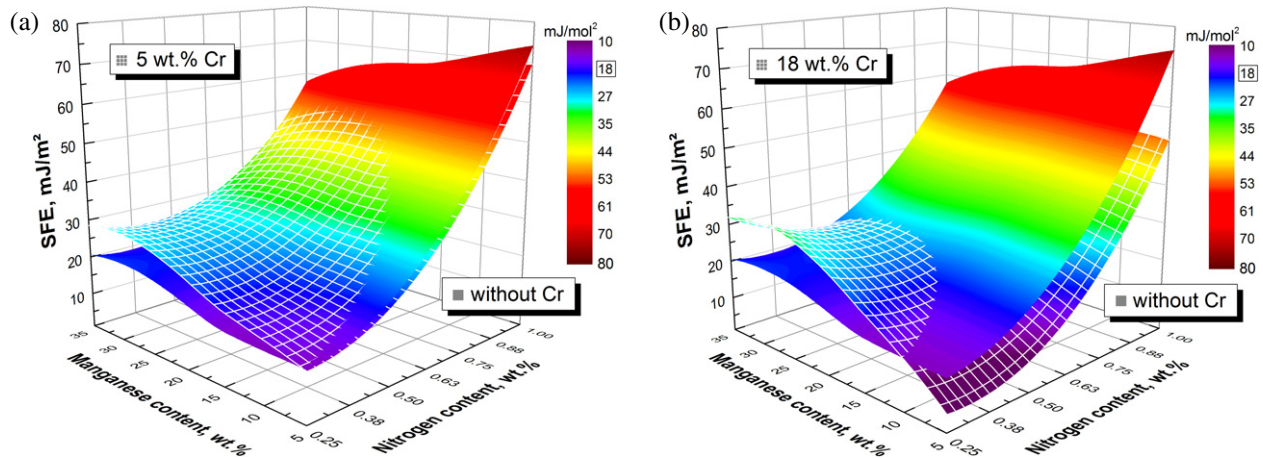
Figure 11. Calculated SFE-maps of Fe–Cr–Mn–N alloys showing the effect of chromium: (a) 5 wt% Cr and (b) 18 wt% Cr.

Fe–15Cr–17Mn with the same manganese content, the SFE value of this alloy matched the applied polynomial description of the low chromium alloys. The effect of manganese content on $\sigma^{\gamma/\varepsilon}$ in the Fe–Cr–Mn–N system was found to be inversely proportional. The obtained values of $\sigma^{\gamma/\varepsilon}$ by Cotes *et al* [83] from the experimental SFE data of Volosevich *et al* [108] and Schumann [109] in the low carbon binary Fe–Mn system show a similar trend of $\sigma^{\gamma/\varepsilon}$. Besides, several authors presume a linear relation of SFE and manganese content in the Fe–Mn system, as also suggested by Nakano and Jacques [33]. The appearance of a minimum in the $\sigma^{\gamma/\varepsilon}$ curve as a function of manganese content in the published data from Volosevich *et al* [108] arises from the corresponding SFE values at room temperature; however, this trend is not corroborated at this time. Using a modified embedded-atom method, Kim *et al* [53] explain the drop in the $\sigma^{\gamma/\varepsilon}$ curve as the result of manganese segregation to the stacking faults in Fe–(10–20 wt%)Mn. However these findings were not experimentally proven. Figure 9 shows calculated SFE values compared with the experimentally measured SFE showing an excellent agreement, which supports the quite reasonable calculation of SFE with a non-monotonous $\sigma^{\gamma/\varepsilon}$. Moreover, the SFE calculation accurately predicts the active deformation mechanism and by that the mechanical fcc phase stability, for a wide range of chemical compositions in the Fe–Cr–Mn–N system.

As can be seen from figure 10, steels with a positive calculated effective Gibbs free energy, $\Delta G^{\gamma \to \varepsilon}$, were expected to have a SFE > 18 mJ m^{-2} which was assigned for the activation of deformation induced twinning, and confirmed the mechanical stability of the γ-phase. For all steels where deformation induced ε- or α'-martensite formation was observed, the calculated $\Delta G^{\gamma \to \varepsilon}$ was found to be negative and the corresponding SFE values were lower than 18 mJ m^{-2}. Compared to these results, the transition between the activation of the TRIP and TWIP mechanism has also been proposed to be at the SFE of 18 mJ m^{-2} by Allain *et al* [60] in Fe–22Mn–0.6C and 15 mJ m^{-2} by Rémy [34] in Fe–5Cr–20Mn–0.5C. At higher SFE values of around 35 mJ m^{-2}, the mechanical twinning will be slightly suppressed and (planar) dislocation glide becomes the

dominant deformation mechanism. A strict division between the SFE values in the TWIP region and pure dislocation glide is not suggested as only a few works in the literature (dark gray dots in figure 10) reported the deformation mechanism to be fully controlled by dislocation glide without mechanical twinning occurring. The corresponding SFE maps at 300 K for the Fe–Mn–N system with the constant chromium contents of 5 and 18 wt% are presented in figures 11(a) and (b), respectively. With increasing manganese and nitrogen content, the SFE increases. Due to the continuous decrease of $\sigma^{\gamma/\varepsilon}$ with increasing manganese content, at higher nitrogen contents the SFE exhibits a slight drop which is more pronounced at lower chromium contents. This trend, however, will just occur for very high SFE levels, where twinning plays a subordinate role as a deformation mechanism. Experimental data on the effect of manganese on SFE in this range of chemical compositions, above all in this system, are not available.

Due to the lack of experimental data, the influence of alloying with chromium on $\sigma^{\gamma/\varepsilon}$ has not been described until now, but the impact of chromium on $\Delta G^{\gamma \to \varepsilon}$ can be assigned to the SFE in Fe–Mn–N system. The effect of chromium on the SFE by calculation agrees with the experimental results in Fe–18Mn–5.6Cr–0.25C [6] for Cr < 10 wt% and in Fe–Cr–Ni [20]. At lower contents, chromium increased the SFE while at higher chromium contents the SFE decreased, which was similar to the values shown by Miodownik [20] in Fe–Cr–Mn. Nevertheless, there are diverse discussions in the literature concerning the effect of chromium on the SFE. According to Ferreira and Müllner [21], with increasing chromium in the Fe–Ni system, the SFE faces a minimum which confirms other studies in the same system by Rhode and Thompson [110] with the minimum at 20 wt% chromium. Other results describe a decreasing effect of chromium (up to 10 wt%) on the SFE in Fe–22Mn–0.6C [61] or Fe–Cr–Ni [25, 111]. Dai *et al* [27] explained this behavior for carbon steels and in the Fe–Mn system instead, and reported that the addition of chromium (or manganese) in small amounts will raise the SFE. Further research is required to confirm any of the latest results regarding the effect of chromium on SFE, especially with a focus on different alloying systems.

Accordingly, the early studies by Lee [106] confirmed that the substitution of nickel by manganese will have a major influence on the activity of chromium in austenitic stainless steels that will affect the austenite stability as well as the mechanical properties.

4. Conclusions and outlook

In this review we have introduced and evaluated the state of the art approaches for SFE calculation by computational thermodynamics in the Fe–Cr–Mn–N system. The currently available thermodynamic data for the calculation of $\Delta G^{\gamma \to \varepsilon}$ accurately define the upper limit of hcp martensite (ε) formation ($\Delta G^{\gamma \to \varepsilon} = 0$ equilibrium line) across a broad range of chemical compositions. In order to consider higher order interactions and the interstitial solid solution of nitrogen on the thermal and mechanical phase stability, the sublattice model has to be applied for the $\Delta G^{\gamma \to \varepsilon}$ calculation, rather than the simplified subregular solution model. It appeared that manganese and nitrogen both stabilize the fcc phase. However, adding chromium to the system results in the stabilization of the fcc phase at low nitrogen contents, while at higher nitrogen contents, the hcp phase becomes more favorable. This can be explained by the thermodynamic description of the hcp phase as Cr_2N nitride. The two common methods for the SFE calculations in the Fe–Cr–Mn–N system using (i) a constant interfacial energy $\sigma^{\gamma/\varepsilon}$ and (ii) including a segregation term, $\Delta G_{\text{segr}}^{\gamma \to \varepsilon}$, to the Gibbs free energy, $\Delta G^{\gamma \to \varepsilon}$, were discussed and found not to suitable reproducing the effect of nitrogen on SFE over a wide range of chemical composition. Therefore, a non-monotonous composition-dependent description of the interfacial energy, $\sigma^{\gamma/\varepsilon}$, was proposed that could be successfully assigned for the activation of deformation-induced twinning in Fe–Cr–Mn–N stainless steels. At the moment, the model validity can be set to the following range of chemical compositions: nitrogen 0.1–1.0 wt%, chromium 0–25 wt%, and manganese 5–30 wt%.

However, further research is required to use the appropriate thermodynamic models and parameters as strong tools to predict and to verify the role of different alloying elements in highly alloyed systems with respect to the phase stabilities and deformation response. Defining the composition-dependency of the driving force for the $\gamma \to \varepsilon$ transformation in high-manganese austenitic steels is necessary. Particularly in higher order systems, the shortage of current thermodynamic datasets may lead to certain inconsistencies in the prediction of the thermodynamic phase stabilities and the available microstructural phases before plastic deformation in more dilute solutions.

The effect of chromium on interfacial energy is not yet clearly described due to the lack of experimental data. Nevertheless, since chromium is known to have a strong interaction with nitrogen leading to the occurrence of short-range ordering, future works must include this element in the model development. The resultant random chromium distribution in the material that was previously reported not to be affected by nitrogen in the iron-matrix [98], as well

as the interaction of chromium with other substitutional elements like manganese, may have a major impact on $\sigma^{\gamma/\varepsilon}$. In addition, the ongoing *ab initio* calculations could be used to support understanding of the composition dependency of the interfacial energy in various systems.

As carbon in Fe–Cr–Mn–N system is of particular interest [18, 23, 51, 101, 112], the development of a carbon-nitrogen di-interstitial [113] thermodynamic model combining the Fe–Cr–Mn–N and Fe–Cr–Mn–C systems is the aim of our future research [18]. The basic approach will be to use the reported assessment of the Fe–C–N system by Herzmann [114] and Du and Hillert [75] which was later re-evaluated by Du [115], where the carbon–nitrogen interaction was considered in the ternary parameter $L_{\text{Fe:C,N}}^{\Phi}$ for the hcp and fcc phases. The thermodynamic description of the hcp phase depending on carbon and nitrogen has to be validated delicately, since the solubility of each interstitial element in the hcp phase is essentially different [116].

Appendix

List of nomenclature

a_γ	...lattice parameter of austenite
a, c	...site numbers in each sublattice
x_i	...molar fraction of element i
va	...vacancies
$y_{i,j}$	...site fractions of the component i, j (i, j = Fe, Mn, Cr)
y_N	...site fraction of nitrogen in the interstitial sublattice with vacancies
y_{va}	...site fraction of vacancies in the interstitial sublattice
G^Φ	...Gibbs free energy of phase Φ
$G_{i:N}^\Phi$	...Gibbs free energy in which all interstitial sites are filled with nitrogen
$G_{i:va}^\Phi$	...Gibbs free energy of the pure elements in a hypothetical nonmagnetic state
G_{excess}^Φ	...contribution to the Gibbs free energy due to the interactions between different elements
L	...interaction parameters in the excess Gibbs energy term
G_{magn}^Φ	...contribution to the Gibbs free energy due to magnetic ordering
T_{Neel}^Φ	...critical temperature for the anti-ferromagnetic ordering
β^Φ	...total magnetic entropy
$\Delta G_{\text{segr}}^{\gamma \to \varepsilon}$	...segregation free energy term
$\Delta G_{\text{chem}}^{\gamma \to \varepsilon}$	...chemical free energy due to Suzuki segregation

$\Delta G^{\gamma\to\varepsilon}_{\text{surf}}$	... surface free energy due to the difference in concentration of nitrogen between matrix and stacking faults
$\Delta G^{\gamma\to\varepsilon}_{\text{elast}}$	... elastic free energy related to the segregation of substitutional and interstitial elements with different atomic sizes
R	... ideal gas constant
Λ_{N}	... interaction energy of nitrogen atoms with dislocations in the fcc structure
x_{N}	... molar fraction of nitrogen in the bulk
$x_{\text{s(N)}}$	... molar fraction of nitrogen at the stacking faults
$\Delta G^{\gamma\to\varepsilon}$	... effective Gibbs free energy for the $\gamma \to \varepsilon$ phase transformation
$\Omega^{\gamma\to\varepsilon}$	... interaction parameter of the excess Gibbs free energy term in the subregular model
SFE	... stacking fault energy
$\sigma^{\gamma/\varepsilon}$	... interfacial energy of the γ/ε-interface
ρ	... molar surface density along {111} planes

References

[1] Lee T H, Shin E, Oh C S, Ha H J and Kim S J 2010 *Acta Mater.* **58** 3173

[2] Saller G, Spiradek-Hahn K, Scheu K C and Clemens H 2006 *Matter. Sci. Eng.* A **427** 246

[3] Kibey S, Liu J B, Curtis M J, Johnson D D and Sehitoglu H 2006 *Acta Mater.* **54** 2991

[4] Huang B X, Wang X D, Wang L and Rong Y H 2008 *Metall. Mater. Trans.* A **39** 717

[5] Bracke L, Mertens G, Penning J, De Cooman B C, Liebeherr M and Akdut N 2006 *Metall. Mater. Trans.* A **37** 307

[6] Bracke L, Penning J and Akdut N 2007 *Metall. Mater. Trans.* A **38** 520

[7] Müllner P, Solenthaler C, Uggowitzer P and Speidel M O 1993 *Matter. Sci. Eng.* A **164** 164

[8] Ilola R J, Hänninen H E and Ullakko K M 1996 *ISIJ Int.* **36** 873

[9] Schramm R E and Reed R P 1975 *Metall. Mater. Trans.* A **6** 1345

[10] Stoltz R E and Vander Sande J B 1980 *Metall. Mater. Trans.* A **11** 1033

[11] Lee Y K 2002 *J. Mater. Sci. Lett.* **21** 1149

[12] Yakubtsov I A, Ariapour A and Perovic D D 1999 *Acta Mater.* **47** 1271

[13] Karaman I, Sehitoglu H, Maier H J and Chumlyakova Y I 2001 *Acta Mater.* **49** 3919

[14] Petrov Y N 2003 *Z. Metallkd.* **94** 1012

[15] Petrov Y N 2005 *Scr. Mater.* **53** 1201

[16] Gavriljuk V, Petrov Y and Shanina B D 2006 *Scr. Mater.* **55** 237

[17] Jandová D, Řehoř J and Nový Z 2004 *J. Mater. Process. Tech.* **157** 523

[18] Lee T H, Ha H Y, Hwang B, Kim S J and Shin E 2012 *Metall. Mater. Trans.* A **43** 4455

[19] Ishida K 1976 *Phys. Status Solidi* A **36** 717

[20] Miodownik A P 1978 *CALPHAD* **2** 207

[21] Ferreira P J and Müllner P 1998 *Acta Mater.* **46** 4479

[22] Curtze S, Kuokkala V T, Oikari A, Talonen J and Hänninen H 2011 *Acta Mater.* **59** 1068

[23] Roncery L M, Weber S and Theisen W 2010 *Metall. Mater. Trans.* A **41** 2471

[24] Mujica L, Weber S and Theisen W 2012 *Mater. Sci. Forum* **706** 2193

[25] Vitos L, Nilsson J O and Johansson B 2006 *Acta Mater.* **54** 3821

[26] Dick A, Hickel T and Neugebauer J 2009 *Steel Res. Int.* **80** 603

[27] Dai Q X, Wang A D, Cheng X N and Luo X M 2002 *Chin. Phy.* **11** 596

[28] Pickering F B 1985 *Proc. of Stainless Steels 84* (The Institute of Metals)

[29] Choi J Y, Ji J H, Hwang S W and Park K T 2011 *Matter. Sci. Eng.* A **528** 6012

[30] Olsen G B and Cohen M 1976 *Metall. Mater. Trans.* A **7** 1897

[31] Adler P H, Olsen G B and Owen W S 1986 *Metall. Mater. Trans.* A **17** 1725

[32] Saeed-Akbari A, Imlau J, Prahl U and Bleck W 2009 *Metall. Mater. Trans.* A **40** 3076

[33] Nakano J and Jacques P J 2010 *CALPHAD* **34** 167

[34] Remy L and Pineau A 1977 *Matter. Sci. Eng.* A **28** 99

[35] Lenel U R and Knott B R 1987 *Metall. Mater. Trans.* A **18** 847

[36] Nylas A and Obst B 1989 *Proc. 1st Int. Conf. on HNS* (The Institute of Metals) pp 194–8

[37] Kitamura Y, Tsuchiyama T, Kikuchi H, Suzuki K and Okamura M 1990 *Proc. 2nd Int. Conf. on HNS* (Stahl und Eisen) pp 171–6

[38] Földéaki M and Ledbetter H 1992 *J. Magn. Mater.* **110** 185

[39] Uggowitzer P J, Magdowski R and Speidel M O 1996 *ISIJ Int.* **36** 901

[40] Vogt J B, Messai A and Foct J 1996 *ISIJ Int.* **36** 862

[41] Onozuka M, Saida T, Hirai S, Kusuhashi M, Sato I and Hatakeyama T 1998 *J. Nucl. Mater.* **255** 128

[42] Tomota Y, Xia Y and Inoue K 1998 *Acta Mater.* **46** 1577

[43] Tomota Y, Nakano J, Xia Y and Inoue K 1998 *Acta Mater.* **46** 3099

[44] Mills D J and Knutsen R D 1998 *Wear* **215** 83

[45] Liu S C, Hashida T, Takahashi H, Kuwano H and Hamaguchi Y 1998 *Metall. Mater. Trans.* A **29** 791

[46] Liu S Y, Liu S C and Liu D 2004 *J. Mater. Sci.* **39** 2841

[47] Sorokina N A and Shlyamnev A P 1999 *Met. Sci. Heat Treat.* **41** 260

[48] Okada H, Sahashi H, Igata N and Miyahara K 2003 *J. Alloys Compounds* **355** 17

[49] Efros N, Korshunov L, Efros B, Chernenko N and Loladze 2004 *Proc. 7th Int. Conf. on HNS* (Steel Grips) pp 391–4

[50] Balitskii A 2004 *Proc. 7th Int. Conf. HNS* (Steel Grips) pp 585–9

[51] Riedner S, Berns H, Tyshchenko A I, Gavriljuk V G, Schulte-Noelle C and Trojahn W 2008 *Mater. wiss. Werkst. Teck.* **39** 448

[52] Lee T H, Oh C S and Kim S J 2008 *Scr. Mater.* **58** 110

[53] Kim S J, Lee T H and Oh C S 2009 *Steels Res. Int.* **80** 467

[54] Hwang B, Lee T H, Park S J, Oh C S and Kim S J 2011 *Mater. Sci. Eng.* A **528** 7257

[55] Hwang B, Lee T H and Kim S J 2011 *Proc. Eng.* **10** 409

[56] Mililtitsky M, Matlock D K, Regully A, Dewispelaere N, Penning J and Hanninen H 2008 *Mater. Sci. Eng.* A **496** 189

[57] Terazawa Y, Ando T, Tsuchiyama T and Takaki S 2009 *Steel Res. Int.* **80** 473

[58] Yang K and Ren Y 2010 *Sci. Technol. Adv. Mater.* **11** 1

[59] Xu M, Wang J, Wang L, Cui W and Liu C 2011 *Adv. Mat. Res.* **146** 26

[60] Allain S, Chateau J P, Bouaziz O, Migot S and Guelton N 2004 *Mater. Sci. Eng.* A **387** 158

[61] Dumay A, Chateau J P, Allain S, Migot S and Bouaziz O 2008 *Mater. Sci. Eng.* **483-84** 184

[62] Saeed-Akbari A, Mosecker L, Schwedt A and Bleck W 2012 *Metall. Mater. Trans.* A **43** 1688

[63] Djurovic D, Hallstedt B V, Appen J and Dronskowski R 2011 *CALPHAD* **35** 479

[64] Lu S, Hub Q M, Johansson B and Vitos L 2011 *Acta Mater.*
59 5728
[65] Sundman B and Ågren J 1981 *J. Phys. Chem. Solids* **42** 297
[66] Nakano J 2013 *Sci. Technol. Adv. Mater.* **14** 014207
[67] De Cooman B C 2011 *Proc. Mater. Res. Soc.* **1296** 1439
[68] Qiu C 1993 *Metall. Mater. Trans.* A **24** 2393
[69] Hillert M and Staffansson L I 1970 *Acta Chem. Scand.*
24 3618
[70] Frisk K 1993 *CALPHAD* **17** 335
[71] Frisk K 1990 *Metall. Mater. Trans.* A **21** 2477
[72] Redlich O and Kister A T 1948 *J. Eng. Chem.* **40** 345
[73] Hillert M and Jarl M 1978 *CALPHAD* **2** 227
[74] Inden G 1982 *Bull. Alloy Phase Diagrams* **2** 412
[75] Du H and Hillert M 1991 *Z. Metallk.* **82** 310
[76] Frisk K 1991 *CALPHAD* **15** 79
[77] Qiu C and Guillermet A F 1993 *Z. Metallk.* **84** 11
[78] Dinsdale A T 1991 *CALPHAD* **15** 317
[79] Feichtinger H, Satir-Kolorz A and Zheng X O 1989 *Proc. 1st
Int. Conf. on HNS* (The Institute of Metals) pp 75–80
[80] Dimova V, Georgiev I, Pechenyakov I and Dobrev R 1978
Mater. Technol. **6** 9
[81] Lee B J 1993 *Metall. Mater. Trans.* A **24** 1919
[82] Simmons J W 1996 *Mat. Sci. Eng.* A **207** 159
[83] Cotes S M, Guillermet A F and Sade M 2004 *Metall. Mater.
Trans.* A **35** 83
[84] Yang H S, Jang J H, Bhadeshia H K D H and Suha D W 2012
CALPHAD **36** 16
[85] Lee Y K and Choi C S 2000 *Metall. Mater. Trans.* A **31** 355
[86] Ishida K 1977 *Scr. Mater.* **11** 237
[87] Holden A, Bolton J D and Petty E R 1971 *J. Iron Steel Int.*
209 712
[88] Guillermet A F and Gustafson P 1985 *High Temp. High
Press.* **16** 591
[89] Andersson J O, Guillermet A F and Gustafson P 1987
CALPHAD **11** 361
[90] Guillermet A F and Huang W 1990 *Int. J. Themophys.*
11 949
[91] Frisk K 1987 *CALPHAD* **11** 127
[92] Qiu C 1993 *Metall. Mater. Trans.* A **24** 629
[93] Huang W 1989 *CALPHAD* **13** 243
[94] Saunders N, Miodownik A P and Dinsdale A T 1988
CALPHAD **12** 351
[95] Anderson J O 1985 *Int. J. Thermophys.* **6** 411
[96] Grujicic M, Nilsson J O, Owen W S and Thorvaldsson T
1988 *Proc. of the 1st Int. Conf. on HNS* (The Institute of
Metals) pp 151–8
[97] Byrnes M L G, Grujicic M and Owen W S 1987 *Acta Mater.*
35 1853
[98] Sumin V V, Chimid G, Rashev T and Saryivanov L 1999
Mater. Sci. Forum **318–320** 31
[99] Gavriljuk V G, Shanina B D and Berns H 2000 *Acta Mater.*
48 3879
[100] Gavriljuk V G, Shivanyuk V N and Shanina B D 2005 *Acta
Mater.* **53** 5017
[101] Gavriljuk V G, Shanina B D and Berns H 2008 *Acta Mater.*
56 5071
[102] Petrov Y N, Gavriljuk V G, Berns H and Escher C 1999 *Scr.
Mater.* **40** 669
[103] Brown L and Thölén A 1964 *Discuss. Faraday Soc.* **38** 35
[104] Santhi Srinivas N C and Kutumbarao V V 1997 *Scr. Mater.*
37 285
[105] Gavriljuk V G, Duz V A, Yefimenko S P and Kvasnevskiy O
G 1987 *Phys. Met. Metallogr.* **64** 84
[106] Lee M C Y 1993 *Metall. Mater. Trans.* A **24** 2379
[107] Nadutov V M 1998 *Mat. Sci. Eng.* A **254** 234
[108] Volosevich P Y, Gridnev V N and Petrov Y N 1976 *Fiz. Met.
Metalloved.* **42** 126
[109] Schumann H 1974 *Krist. Tech.* **9** 1141
[110] Rhode C G and Thompson A W 1977 *Metall. Mater. Trans.* A
8 1901
[111] Otte H M 1957 *Acta Metall. Mater.* **5** 614
[112] Ha Y H, Lee T H, Oh C S and Kim S J 2009 *Scr. Mater.*
61 121
[113] Ko C and McLellan R B 1989 *J. Phys. Chem. Solids* **50** 619
[114] Hertzmann S 1987 *Metall. Mater. Trans.* A **18** 1753
[115] Du H 1993 *J. Phase Equilib.* **14** 682
[116] Naumann F K and Langenscheid G 1965 *Arch.
Eisenhuttenwes.* **36** 677